The Fifth International Workshop on Micro and Nanotechnology for Power Generation and Energy Conversion Applications
PowerMEMS 2005
Nov. 28-30, 2005
Takeda Hall, The University of Tokyo, Tokyo, Japan

DEVELOPMENT OF HIGH-SPEED BEARINGS FOR MICRO GAS TURBINES -STABILITY ANALYSIS OF FOIL BEARINGS

P. Vleugels, T. Waumans, J. Peirs, F. Al-Bender, D. Reynaerts
Katholieke Universiteit Leuven, Department of Mechanical Engineering
Celestijnenlaan 300B, B-3001 Leuven, Belgium
Dominiek.Reynaerts@mech.kuleuven.ac.be

Abstract

Mesoscopic or micro gas turbines can be an interesting replacement for batteries. A drawback of this downscaling is the increased rotor speed in the order of 500.000 rpm, which makes the bearing design a challenging task. Air bearings are the only type of bearing which can withstand the severe circumstances of high speed and high temperature. However air bearings and more in particular aerodynamic bearings are prone to instabilities. Therefore more advanced bearing types like foil bearings are an interesting solution. This paper shows simulations to predict the static behaviour of a foil bearing. Furthermore, a method to calculate the dynamic properties is proposed. Using these stiffness and damping coefficients a stability analysis is carried out. This analysis shows that, even without additional damping, a foil bearing is more stable than a normal aerodynamic journal bearing but not as stable as is hitherto believed. However, due to its flexible nature, it is possible to improve the stability by simple means.

Keywords: PowerMEMS, micro foil bearings, bearing stability, micro gas turbine

1 INTRODUCTION

A miniature gas turbine is under development for application in small portable power generators, producing electrical energy from fuel.
The main parts of the power unit are the compressor, turbine, combustion chamber and generator. First prototypes [1] have been built and tested but performance and efficiency are clearly limited by the maximum speed limit of the ball bearings (only 100.000 rpm), lower than the targeted speed of 500.000rpm. Current research focuses on the design and manufacturing of a bearing which can be used up to 500.000 rpm. In parallel, other project partners are developing the combustion chamber, heat recuperator, generator and monitoring system.

2 BEARING CHOICE

In order to keep the pressure ratio constant, the rim speed of the compressor should be kept constant, which results in a high rotational speed (500,000 rpm and higher) when downscaling. Keeping also the high temperatures (between 100°C and 1000°C depending on the location) in mind this quickly limits the choice to air bearings. Air bearings can be divided into aerodynamic (or self-acting) bearings, aerostatic (or externally pressurised) bearings, and hybrid bearings that are a combination of both. Aerostatic bearings require a constant supply of pressurised air to operate. This means that a reservoir of compressed air is required during start-up and that compressed air has to be tapped from the compressor during operation. Aerodynamic bearings generate the required bearing forces through the relative movement between the rotor and bearing surfaces. Thus no extra 'energy' supply is required (although energy is lost through viscous friction as for all air bearings). The main drawbacks of aerodynamic bearings are that they go through a phase of dry friction during starting up and stopping down, and that they are generally less dynamically stable than aerostatic bearings.
Foil bearings are a type of aerodynamic bearings which are becoming very popular and being under research by famous institutes like NASA, Turbo Texas A&M University [2], MiTi [3] and Tokyo University [7]. However, most publications focus on experimental work without much theoretical work or design guidelines, which makes it difficult to scale down current designs to the desired size of approximately 6 mm diameter. It is even often unclear why a certain design works well and where its operation limits are. This paper is an attempt to analyse the dynamic behaviour of a foil journal bearing.

3 FOIL BEARING MODEL

Although foil bearings (see Figure 1) are complex systems consisting of an air film, a top foil, a flexible structure and in some cases a damping source (e.g hysteric friction or special coatings) it is possible to simulate them quite easily. A very popular model was first published by Heshmat [3] and is still in use. In this model the top foil is modelled as an ideal top foil: stiff enough to have no "sag" between the bumps or springs but without membrane stresses. This means that the deflection at each point only depends on the forces acting on the particular point. The assumption of no membrane stresses is disputable because the top foil is bent into a shell which gives it stiffness in the axial direction [4]. However, the assumption of an ideal top foil is still widely used and therefore it is adopted here too to make the simulations easy to compare with former simulations [5]. As a flexible structure, one can take different elements like corrugated

foils or bump foils [3], advanced elastic materials [6] or spaced double wounded foils [7]. Nevertheless the modelling remains the same, the flexible structure is modelled as a set of springs, with or without dampers in parallel. T he flexible element enters the normalized Reynolds equation, shown in (1), for aerodynamic bearings via the pressure dependent gap height H, where the α parameter is inversely proportional to the surface stiffness K and the ambient pressure p_a, and proportional to the clearance C. The rotational frequency is denoted by ω.

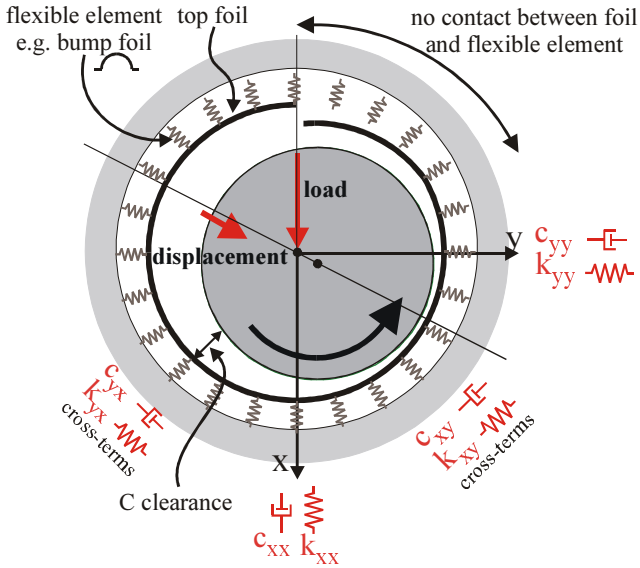

Figure 1 Foil journal bearing scheme

$$\frac{\partial}{\partial X}\left(P(H+\alpha(P-1))^3\frac{\partial P}{\partial X}\right)+\frac{\partial}{\partial Y}\left(P(H+\alpha(P-1))^3\frac{\partial P}{\partial Y}\right)=(1)$$

$$\Lambda\frac{\partial}{\partial X}\left(P(H+\alpha(P-1))\right)+\sigma\frac{\partial}{\partial T}\left(P(H+\alpha(P-1))\right)$$

$$\Lambda=\frac{6\mu\omega}{p_a}\left(\frac{R}{C}\right)^2 \quad \sigma=\frac{12\mu\omega\gamma}{p_a}\left(\frac{R}{C}\right)^2 \quad \gamma=\frac{\omega_w}{\omega}$$

$$X=\frac{x}{C} \quad Y=\frac{y}{C} \quad P=\frac{p}{p_a} \quad T=\omega t \quad \alpha=\frac{C}{Kp_a} \qquad (2)$$

4 STATIC PROPERTIES OF FOIL BEARINGS

The static solution can be found by removing the σ term in (1). The resulting equation can be solved by a numerical scheme as presented by Heshmat [3]. This method consists of solving the equation by finite differences using the Newton Raphson method. However, care should be taken for the boundary conditions of the foil bearing problem. As the top foil is in general not fixed to the flexible element, it comes loose when sub-ambient pressure is reached. This problem is analogues to cavitation, which takes place in liquid hydrodynamic journal bearings. At the angle θ_b where the pressure becomes sub-ambient, this gives the following boundary conditions:

$$P=1 \qquad \frac{\partial P}{\partial X}=0 \text{ at } X=R\theta_b \qquad (3)$$

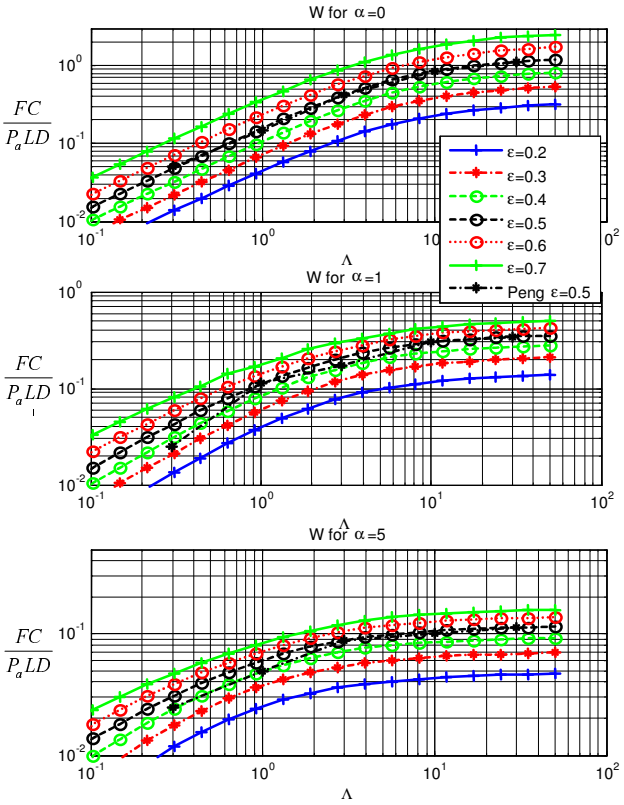

Figure 2 Static load capacity of journal foil bearings (in comparison with Peng et al. [5])

These conditions are also known as the Reynolds or JFO boundary conditions. From angle θ_b on, the gap height H remains constant. Numerical problems arise because this angle θ_b (and the corresponding height) is not known beforehand. A correct implementation of these boundary conditions involves an additional step in each iteration, which consists in setting the gap height equal to the gap at θ_b. After some iterations the boundary condition will be fulfilled because there is no pressure generation anymore so that the pressure derivative is equal to zero. Another often used method consists of setting the sub-ambient pressure equal to 1. This method does not fulfil the correct boundary conditions.

Figure 2 shows the load capacity for foil bearings with α values 0, 1 and 5 as function of bearing number Λ and eccentricity ε. The case of α=0 can be seen as a normal fixed-geometry aerodynamic bearing with a pressure groove on top and without the sub-ambient region. Important to notice is the totally different scale of the load. The load capacity for the same eccentricity is greatly reduced. However, the generated pressure will increase the gap such that the minimal gap is larger than (1-ε)C. In this way, it is much more feasible to choose a high eccentricity value as working point (in particular >1). As the bearing contains a flexible element it is more "forgiving" to hard contact between the rotor and bearing surface (e.g. due to a suddenly increased load). Top foil coatings even improve this property.

5 DYNAMIC PROPERTIES OF FOIL BEARINGS

A major problem with aerodynamic bearings and fluid film bearings in general is their dynamic stability. The static solution does not give information about the dynamic stability at a certain working point. It is known from literature that especially aerodynamic bearings are prone to half-speed whirl, a self-excited vibration which results in undamped whirling at approximately half the rotational frequency. In order to evaluate stability, the stiffness and damping properties should be known. The method of perturbation, see (4), is usually adequate for calculation of 4 stiffness and 4 damping coefficients. These consist of direct and cross-coupled coefficients. The K_{xx}, K_{yx}, C_{xx} and C_{yx} can be calculated with a perturbation in X-direction, K_{yy}, K_{xy}, C_{yy} and C_{xy} with a perturbation in Y-direction. As will be shown later, the cross-coupling terms are a major source of instability.

$$P = P_0 + \kappa e^{i(\tau+\varphi)} \quad H = H_0 + \eta e^{i\tau} \quad K = \frac{\kappa}{\eta}\cos\varphi \quad C = \frac{\kappa}{\eta}\sin\varphi \tag{4}$$

$$\nabla\left[\left(3P_0G_0^2 - \Lambda P_0\right)\eta + \left(3P_0G_0^2\alpha\nabla P_0 + G_0^3\nabla P_0 - \Lambda(P_0\alpha + G_0)\right)K + P_0G_0^3\nabla K\right] = -\sigma(G_0 + P_0\alpha)C$$

$$\nabla\left[\left(3P_0G_0^2\alpha\nabla P_0 + G_0^3\nabla P_0 - \Lambda(P_0\alpha + G_0)\right)C + P_0G_0^3\nabla C\right] = \sigma(P_0\eta + (G_0 + P_0\alpha)K$$

$$G_0 = H_0 + \alpha(P_0 - 1)$$

Figure 4 shows the synchronous K_{xx} and K_{xy} coefficients for three different α values: 0, 1 and 5. The α value has a large impact on the range and influences also the general trend of the values. The figures show that the flexible element is predominant from a certain bearing number Λ (or speed) on, which is not so surprising if one keeps in mind that the calculated stiffness consists of the air film stiffness and the flexible element stiffness in series. The point where this occurs shifts to the left when the α value is increased. This behaviour is also clearly noticeable in the other direct stiffness term K_{yy} (not shown) and less in the cross-coupling terms K_{xy} and K_{yx} (not shown). The damping coefficients are also calculated and used for further stability simulations. The obtained values of the synchronous stiffness and damping coefficients agree very well with the values published by Peng et al. [5].

6 STABILITY ANALYSIS

Using the previously mentioned perturbation method it is possible to calculate the stiffness and damping properties of the bearings. For a symmetric system with a rigid rotor this gives the system matrix shown in (5). The stability of this system can be evaluated by supposing that the shaft is whirling and then looking for the whirl frequency $\gamma\omega$. Finally the Routh-Hurwitz stability criterion can be used for this. Nevertheless, it is more useful to normalize the equation as initially proposed by Lund [8], as shown in (6) , because a very important parameter, the critical mass "M_c" is introduced.

Using these normalisations, an equivalent stiffness K_{eq} and a stability criterion can be defined as shown in (7). A major problem with these equations is their dependency on the whirl frequency $\gamma\omega$, so that we have to use an iterative method of solution to find γ.

$$M\begin{bmatrix}\ddot{x}\\ \ddot{y}\end{bmatrix} + \begin{bmatrix}c_{xx} & c_{xy}\\ c_{yx} & c_{yy}\end{bmatrix}\begin{bmatrix}\dot{x}\\ \dot{y}\end{bmatrix} + \begin{bmatrix}k_{xx} & k_{xy}\\ k_{yx} & k_{yy}\end{bmatrix}\begin{bmatrix}x\\ y\end{bmatrix} = 0 \tag{5}$$

$$M_c = \frac{M\,p_a}{\mu^2 L\left(\frac{R}{C}\right)^5} = \frac{K_{eq}}{72\Lambda^2} \qquad K_{ij} = \frac{k_{ij}C}{p_aLD} \qquad C_{ij} = \frac{c_{ij}C\omega}{p_aLD} \tag{6}$$

This parameter is taken into account during the calculation of the stiffness and damping coefficients via the σ-parameter which makes it absent in the final equations. At the end the critical mass can be calculated using K_{eq} and Λ using (6).

$$K_{eq} = \frac{K_{xx}C_{yy} + K_{yy}C_{xx} - K_{xy}C_{yx} - K_{yx}C_{xy}}{C_{xx} + C_{yy}} \tag{7}$$

$$(K_{eq} - K_{xx})(K_{eq} - K_{yy}) - K_{xy}K_{yx} - C_{xx}C_{yy} + C_{xy}C_{yx} = 0$$

Important to notice is the 5th power in the M_c parameter, which indicates that the R/C ratio is very important but also that a slightly different clearance value C, e.g. due to manufacturing errors or thermal expansion, can have a serious impact on the bearing stability. A closer look at K_{eq} and the stability criteria reveals that the cross-coupling terms of the stiffness are a major source of instability. Prudence is called for in the evaluation during whirling. The whirling itself can be stable due to non-linearities which can induce sufficient additional damping to stabilize the whirling.

7 STABILITY SIMULATIONS

Using the previously mentioned techniques, it is possible to calculate stability maps as shown in Figure 3. These maps relate M_c, Λ and load W with each other, e.g. if the bearing geometry and rotor mass are fixed, W and M_c can be calculated as a function of Λ and the crossing of both lines determines the maximum bearing number Λ or the maximum speed. The lines of constant eccentricity ε are also shown as they are used for the calculation of the stability map.

In order to make the stability region as large as possible, the critical rotor mass should be as small as possible. However, the load W (often just the weight) should be as large as possible, often conflicting with the requirement of low M_c. The determining factor for the critical rotor mass is the C/R-ratio which should be small. Typically it has a value of 10^{-3}. For shafts with a diameter in the order of 6 mm this results in a clearance of 3 µm. Due to limitations in manufacturing capabilities, this is very hard to reach for mesoscopic or micro bearings. However, for a clearance of 10 µm (thus a C/R-ratio of $3.33\ 10^{-3}$) M_c becomes a factor 411 worse.

Figure 3 shows the stability maps for foil bearings with α values 0, 1 and 5. There is only little difference between the maps with α-value 0 (almost comparable with a fixed geometry journal bearing with pressure groove) and the foil bearings with α-value 1 and 5. A comparison with the map for a normal plain journal bearing [9] reveals that the maximum speed is only increased with only 50% to 100%, not fully in line with literature where almost "unlimited" speed is promised.

However, foil bearings can safely operate at higher eccentricities compared to normal fixed geometry journal bearings, as mentioned before. This makes it possible to e.g.

decrease the clearance value C, lowering the M_c value drastically and consequently increasing the maximum achievable speed.

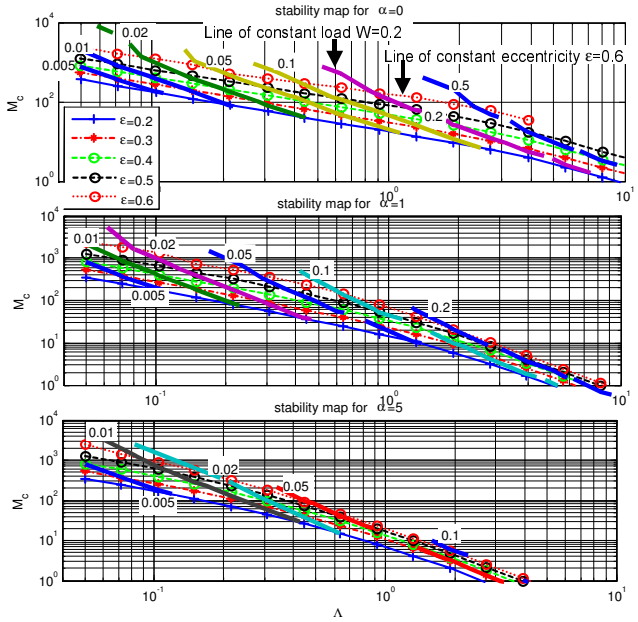

Figure 3 Stability maps

The stability can also be improved by increasing the load which is not so difficult in a foil bearing. For instance putting a shim between the bearing housing and the flexible element, in a way that the top foil is not perfectly cylindrical anymore, can be sufficient (known as geometrical preload). Also additional damping sources (e.g. a layer of rubber or bump friction dissipation) can be added to improve the stability.

8 FUTURE RESEARCH

Up to now the results are based on simulations. Future research will consist of experimental work in order to validate the simulations. Also further refinement (e.g. taking the membrane stresses into account) of the model will be carried out.

9 CONCLUSION

A model and a technique to calculate the load capacity and dynamic stiffness and damping properties of aerodynamic foil bearings is presented. Simulations show that both the absolute value and the general trend of the stiffness are highly influenced by the flexibility parameter α. Based on these coefficients a stability analysis is carried out, which results in stability maps for foil bearings. These maps show that the stable behaviour of foil bearings is limited in speed too. However, due to its flexible nature, it is possible to reduce the C/R-ratio and to increase the load on the bearings, leading to an increased achievable speed.

10 REFERENCES

[1] J. Peirs et al,"Development of an axial microturbine for a portable gas turbine generator", J. Micromech. Microeng. 13 (2003), pp. 190-195

[2] T. Ho Kim, L. San Andres, "Heavily Loaded Gas Foil Bearings: a Model Anchored to Test Data", Proc. of GT2005, Reno-Tahoe, Neveda, USA, GT2005-68486

[3] H. Heshmat et al,"Analysis of Gas-Lubricated Foil Journal Bearings", Journal of Lubrication Technology, 105, pp. 647-655

[4] M. Carpino et al,"Effect of Membrane Stresses in the Prediction of Foil Bearing Performance", Tribology Transactions, 37 (1994),1, pp. 43-50

[5] J.P. Peng, M. Carpino,"Calculation of Stiffness and Damping Coefficients for Elastically Supported Gas Foil Bearings", Journal of Tribology, 115,20-27

[6] Hou, Y et al,"Comparative test on two kinds of new compliant foil bearing for small cryogenic turbo-expander", Cryogenics, 44 (2004), pp. 69-72

[7] Kitazawa, S et. al,"Prototyping of Radial and Thrust Air Bearing for Micro Gas Turbine", Proc. of IGTC2003, Tokyo, TS-019

[8] J.W. Lund,, "The Stability of an Elastic Rotor in Journal Bearings With Flexible, Damped Supports », Journal of Applied Mechanics, pp 911-920, 1965

[9] D. F. Wilcock (Editor), "Design of Gas Bearings", M.T.I. Inc, Latham NY 1969

11 ACKNOWLEDGEMENT

This research is sponsored by the IWT, the Institute for the Promotion of Innovation by Science and Technology in Flanders, Belgium, project SBO 030288 "PowerMEMS", and by the Belgian programme on Interuniversity Poles of Attraction (IAP5/06: AMS). The authors assume the scientific responsibility of this paper.

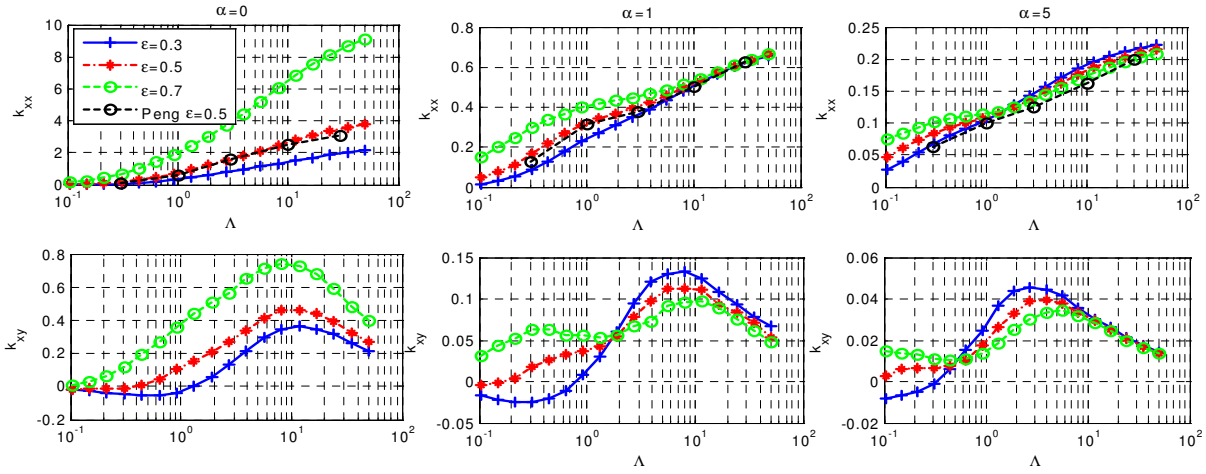

Figure 4 Synchronous stiffness coefficients for different α values